Batteries & Supercaps

Research Article
doi.org/10.1002/batt.202400107

Chemistry Europe
European Chemical Societies Publishing

www.batteries-supercaps.org

Understanding the Effects of Bi Modification on the Properties of Ni-Rich Cathodes

Zifei Meng,[a] Jiahui Hou,[a] Panya Thanwisai,[a] Jinzhao Fu,[a] Zeyi Yao,[a] Yadong Zheng,[a] Wenting Jin,[a] Zexin Wang,[a] Zhenzhen Yang,[b] Xiaotu Ma,*[a] and Yan Wang*[a]

With the skyrocketing market demands for energy storage, lithium ions batteries (LIB) with higher energy density are urgently needed. Cathodes play a critical role in determining the energy density of LIB, and the most popular one is Ni-rich cathode due to its high capacity. However, due to the fast structural degradation, Ni-rich cathode materials should be further modified to achieve higher stability. Herein, we introduce bismuth ions in $LiNi_{0.83}Co_{0.11}Mn_{0.06}O_2$ cathodes by adding Bi_2O_3 during sintering to optimize the specific capacity and cycle stability. By adding 0.1 % mol Bi, the Li^+ diffusion and structural stability are effectively optimized, leading to improved electrochemical performances. The modified sample delivers much higher specific capacity (222.9 $mAhg^{-1}$, 0.05 C) than unmodified sample (204 $mAhg^{-1}$, 0.05 C). Meanwhile, the specific capacity of optimized sample after 100 cycles at 0.33 C is 27.75 $mAhg^{-1}$ higher than that of unmodified sample. Therefore, this work demonstrates that Bi modification can be regarded as a possible solution to optimizing the electrochemical performance of Ni-rich cathodes.

1. Introduction

The skyrocketing demands of LIB is motivated by the popularity of electric vehicles during recent decades due to the high energy density of LIB.[1] To meet the rapid growing of the requirement for energy storage, the performance of LIB should be further improved. Cathode materials can significantly influence the energy and power density of LIB, acting as the major performance-limiting factor.[2] Many cathode materials have been developed, such as Ni-rich, Mn-rich and Li-rich oxide materials.[3–5] However, these cathode materials often face fading issues, like structure degradation.[6–8] The structure degradation is mainly caused by the structure collapse and the irreversible phase transition during lithiation/delithiation process, leading to fast capacity fading.[9–11] Meanwhile, the poor stability of structure can also cause low capacity at high rates.[12,13] Therefore, the structure stability of cathode materials is emergent to be optimized.[14,15] Different modification strategies have been employed to improve the structure stability, like controlling the exposed facets and morphology of primary particles, optimizing the solid electrolyte interphase (SEI), and synthesizing single crystal shapes.[16–18]

Doping and coating are the most popular modification strategies because they are significantly effective and can be simply achieved during synthesis process.[19–21] Zhou et al. proposed that Bi_2O_3 at surface can hinder the migration of oxygen ion vacancies and reduce the irreversible loss of oxygen and thus optimize the structure stability and improve Li^+ diffusion of $Li_{1.2}Mn_{0.54}Ni_{0.13}Co_{0.13}O_2$, achieving high cycle and rate capability.[22] Hao et al. also claimed that Bi ions can optimize the interfacial stability. With 0.07 mol % Bi doping, the capacity and cyclability of LMO can be optimized, and the capacity retention of Bi modified sample is 54.3 $mAhg^{-1}$ higher than that of unmodified sample.[23] However, Bi_2O_3 has not been employed as a dopant in polycrystal Ni-rich cathode materials to improve the electrochemical performance. $Bi(NO_3)_3$ has only been used to optimize the synthesis process of single crystal $LiNi_{0.6}Co_{0.2}Mn_{0.2}O_2$, and Bi ions can lower the sintering temperature because Bi ions gather at the gain boundary and accelerate the diffusion and fusion of primary particles during synthesis process. However, the specific capacity of Bi modified samples are much lower than that of unmodified sample.[24] Therefore, whether Bi_2O_3 can be regarded as possible doping or coating materials to optimize the properties of Ni-rich cathode materials is still unclear.

Herein, in this study, we study the impacts of Bi substitution on the crystal structure and electrochemical performance of the Ni-rich cathodes. By introducing Bi ions, the electrochemical performance of NMC cathode materials has been significantly improved. Especially for the NMC cathode modified with 0.1 mol % Bi (1BiNMC), it delivers the best electrochemical performance in both rate and cycling tests. The specific capacity of 1BiNMC at 0.05 C is 18.9 $mAhg^{-1}$ higher than VNMC and with higher rate, 5 C, it is 43.4 $mAhg^{-1}$ higher than VNMC. Meanwhile, the capacity retention of 1BiNMC is 87.44 % after 100 cycles at 0.33 C, ~10 % higher than VNMC. As revealed by various characterizations, Bi substitution can not only lower the cation mixing but also can limit contraction in c-direction to reinforce structural stability and prevent the formation of

[a] Z. Meng, J. Hou, P. Thanwisai, J. Fu, Z. Yao, Y. Zheng, W. Jin, Z. Wang, X. Ma, Y. Wang
Department of Mechanical and Materials Engineering, Worcester Polytechnic Institute, Worcester, MA-01609, USA
E-mail: xma3@wpi.edu
yanwang@wpi.edu

[b] Z. Yang
Chemical Sciences and Engineering Division, Argonne National Laboratory, Lemont, IL-60439, USA

Supporting information for this article is available on the WWW under https://doi.org/10.1002/batt.202400107

Research Article
doi.org/10.1002/batt.202400107
Chemistry Europe
European Chemical Societies Publishing

cracks. Altogether, our work demonstrates that Bi modification can be regarded as a possible solution to optimizing the electrochemical performance of Ni-rich cathodes.

2. Results and Discussions

2.1. Morphology and Crystallinity

The morphology of VNMC, 1BiNMC, and 3BiNMC are observed through SEM, as shown in Figure a–c. Secondary particles in all samples are spheres and the particle size distribution of all samples are similar. However, the difference in the primary particle size among the three samples is obvious, and the primary particle size decreases with higher concentration of Bi ions. The primary particle size of VNMC is around 300 nm. For 1BiNMC, the primary particles are almost 250 nm with a little 300 nm particles. In 3BiNMC, the primary particles are around 150 nm, much less than that of VNMC and 1BiNMC. The chemical bonds between Bi and nonmetals are stronger than those in NMC and when Bi ions were added during synthesizing NMC and diffuse into the precursors, they can suppress the growth of primary particles in the precursor and cause small primary particles in the obtained cathode materials.[25] Thus, for 1BiNMC, the primary particle size is only around 50 nm smaller than VNMC while for 3BiNMC, the primary particle size is around half of that in VNMC. The smaller primary particles can reduce the Li^+ diffusion path length and lead to a denser stacking structure, which helps prevent the breakdown of secondary particles.[25] The elemental distribution of VNMC, 1BiNMC, and 3BiNMC is examined by the EDX mapping. The particle microstructure of VNMC and 1BiNMC is investigated by cross-sectional SEM, as shown in Figure S1. Primary particles in VNMC are randomly oriented while for 1BiNMC, primary particles tend to be radially oriented. The radial orientation of primary particles allows short Li^+ diffusion path from bulk to surface in secondary particles, enabling higher diffusion coefficient and better rate performance. In Figure 1d–i, S2 and S3, Ni, Mn, Co, and O elements are distributed uniformly in all samples. Meanwhile, the uniform distribution of Bi on 3BiNMC can be observed in Figure 1e.

2.2. Composition and Structure

The results of ICP-MS indicate that the Bi modified NMC cathodes were synthesized successfully with the desired composition (Table S1). The percentage of Mn and Co matches the designed composition while only the percentage of Ni ions decreases with the increasing percentage of Bi ions, indicating

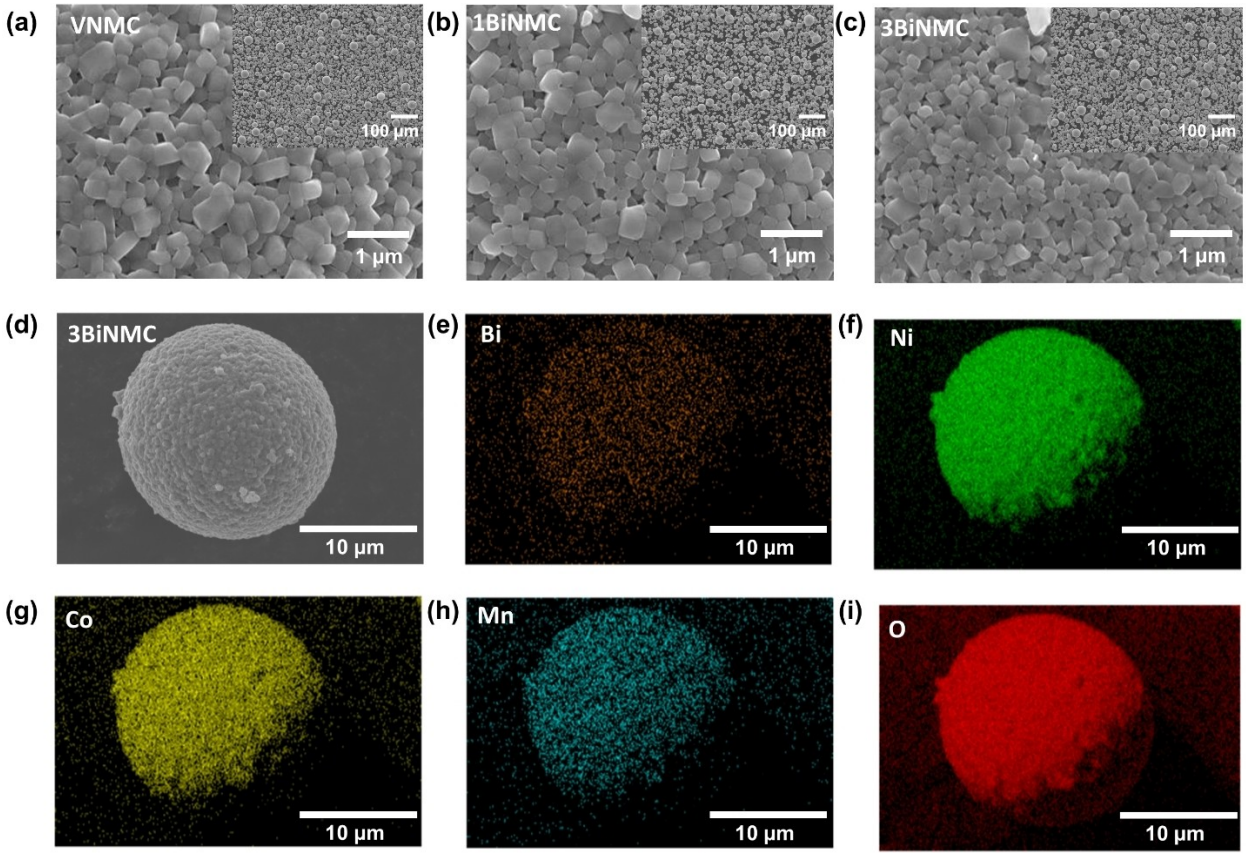

Figure 1. Morphology and elemental distribution of VNMC, 1BiNMC, and 3BiNMC. (a–c) SEM image of VNMC, 1BiNMC, and 3BiNMC; (d–i) EDX mappings image of 3BiNMC; The inset in (a) presents the low magnification SEM image of VNMC; The inset in (b) presents the low magnification SEM image of 1BiNMC; The inset in (c) presents the low magnification SEM image of 3BiNMC.

Research Article
doi.org/10.1002/batt.202400107
Chemistry Europe
European Chemical Societies Publishing

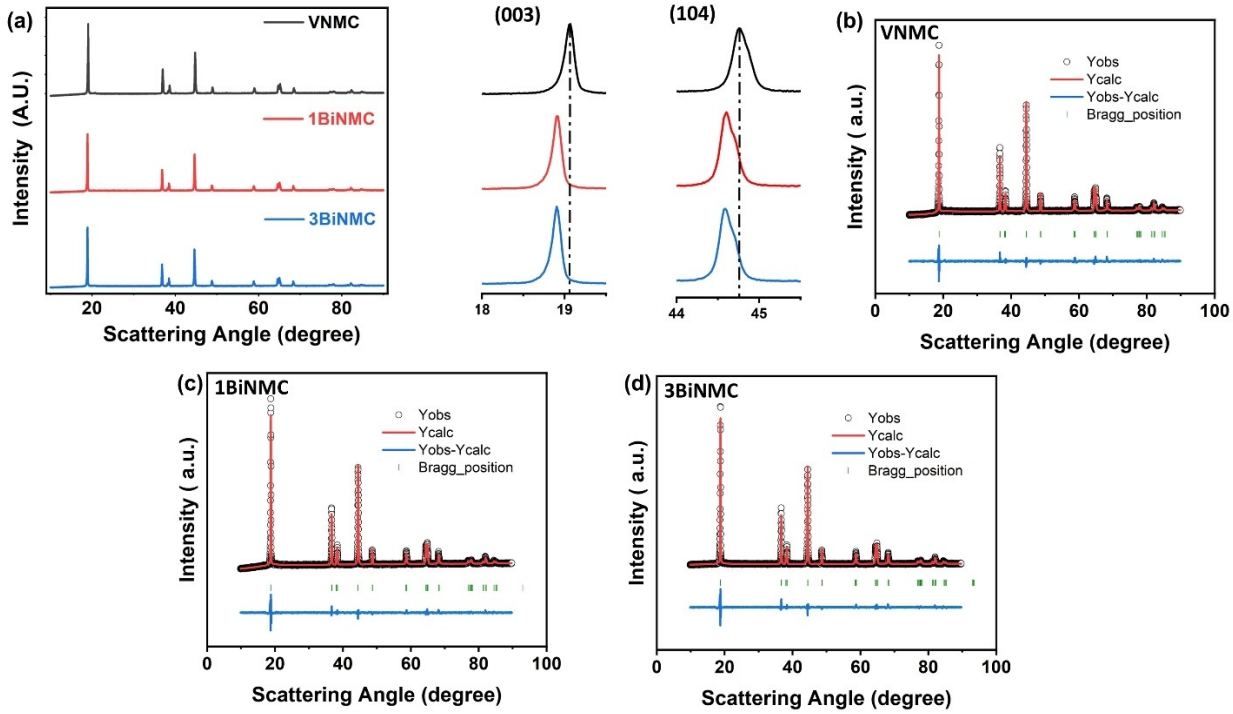

Figure 2. The structure information of VNMC, 1BiNMC, and 3BiNMC. (a) X-ray diffraction patterns and their (003) and (104) planes of VNMC, 1BiNMC, and 3BiNMC; (b–d) Refinement profile of VNMC, 1BiNMC, and 3BiNMC.

that the sites of Ni ions were occupied by Bi ions. Meanwhile, according to the XRD results in Figure 2a, there are no impurity phases and the clear splitting of (108)/(110) and (006)/(102) peaks indicates the well crystalline layered structure of all samples.[26,27] However, because the radius of Bi ions are larger than that of other transition metal ions, Bi ions are able to cause lattice expansion.[28] In Figure 2a, the (003) and (104) peaks of Bi modified NMC cathodes shift to the left, indicating the lattice expansion in 1BiNMC and 3BiNMC.[29,30] The corresponding lattice expansion is also investigated by the XRD refinement results in Figure 2b–d and Table 1. The expansion of lattice can broad the Li^+ diffusion path, causing faster Li^+ diffusion and better rate performance.[31] The cation mixing in the Li layer also can be obtained from the XRD refinement results, and cation mixing of 1BiNMC and 3BiNMC are 4.49% and 4.55%, respectively. Both of them have lower cation mixing than VNMC(4.76%), which representing the highly ordered layered structure.[29] Because of the low cation mixing and highly ordered layered structure, optimized specific capacity and cycle stability can be achieved.[32]

Table 1. Refinement data of VNMC, 1BiNMC, and 3BiNMC.

Sample	a/b-axis (Å)	c-axis (Å)	Volume ($Å^3$)	Ni in Li layer (%)	χ^2	Rwp (%)
VNMC	2.8709	14.1941	101.312	4.76%	5.67	2.72
1BiNMC	2.8730	14.2030	101.528	4.49%	5.09	2.60
3BiNMC	2.8761	14.2184	101.858	4.55%	7.50	5.48

To determine the functions of Bi ions on the surface chemical states of NMC, the high-resolution XPS spectra of Bi 4f, Ni 2p3/2 and O 1s are analyzed and the results are shown in Figure 3 and S4. Specifically, two Bi 4f peaks, observed at around159.2 eV and 164.5 eV, are characteristic of Bi^{5+} ions, as illustrated in Figure 3a.[23] Meanwhile, as shown in Figure S4, Bi can be detected in both surface and bulk. The intensity of Bi on the surface is higher than that at the bulk, indicating that the Bi modification contains both Bi doping and Bi_2O_3 coating. As shown in Figure 3b, in Ni $2p_{3/2}$ spectra, there are four peaks: the two peaks the Ni^{2+} and Ni^{3+} ions (856 and 854 eV) while the other two are the satellite peaks (861 and 865 eV).[27] According to the Ni 2p3/2 spectrum of VNMC, 1BiNMC, and 3BiNMC, the percentages of Ni^{2+} and Ni^{3+} ions in each sample are calculated. As shown in Figure 3c and Table S2, 1BiNMC and 3BiNMC contain less Ni^{2+} but more Ni^{3+} ions than VNMC. Especially, the differences of the percentages of Ni^{2+} and Ni^{3+} ions in VNMC and 1BiNMC are obvious. The lower content of Ni^{2+} can be attributed to the similar ionic radii of Bi^{5+} (74 Å) and Ni^{2+} (72 Å), which allows Bi^{5+} to occupy the sites of Ni^{2+}.[33] Higher content of Ni^{2+} ions can cause higher Li^+/Ni^{2+} disorder in Ni-rich cathode materials, and the cation mixing in VNMC should be higher than that of 1BiNMC, which is corresponding to the result in XRD refinement.

Meanwhile, O1s spectra (Figure 3d) contain two peaks at 531.9 eV and 529.5 eV. The peak at 531.9 eV represents active oxygen species (Li_2CO_3 and LiOH), while The peak at 529.5 eV is attributed to the lattice oxygen bound to metals.[34] Figure 3e and Table S4 demonstrate the percentage of the two peaks. 1BiNMC and 3BiNMC have higher content of lattice oxygen

Research Article
doi.org/10.1002/batt.202400107
Chemistry Europe
European Chemical Societies Publishing

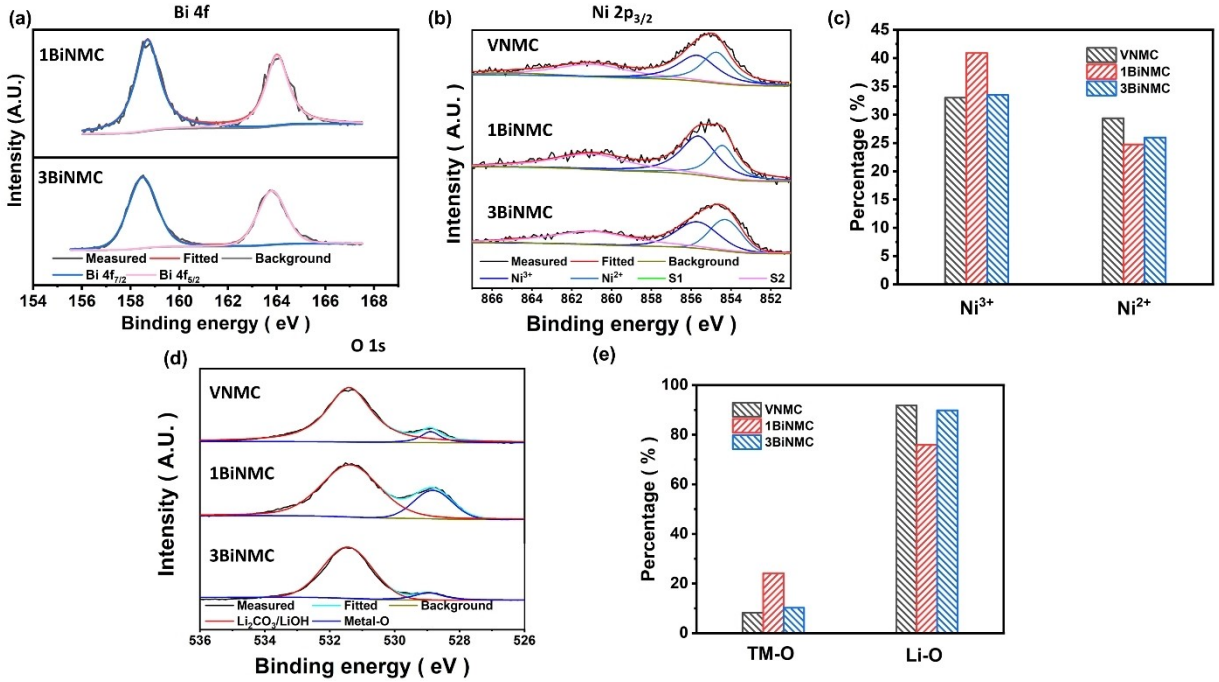

Figure 3. The surface chemical states of elements in VNMC, 1BiNMC, and 3BiNMC. (a) High-resolution XPS spectra of Bi 4f in 1BiNMC, and 3BiNMC; (b) High-resolution XPS spectra of Ni $2p_{3/2}$ in VNMC, 1BiNMC, and 3BiNMC; (c) Percentage of Ni^{2+} and Ni^{3+} ions in VNMC, 1BiNMC, and 3BiNMC; (d) High-resolution XPS spectra of O 1s in VNMC, 1BiNMC, and 3BiNMC; (e) Percentage of peaks of O 1s in VNMC, 1BiNMC, and 3BiNMC.

bound to metals and less active oxygen species, indicating that the residual lithium can be effectively reduced by Bi_2O_3 coating on the surface and the serious side reaction between cathode and electrolyte can be limited.[18] As for Co 2p and Mn 2p, their XPS spectra are also carried out and displayed in Figure S5. There are no obvious position shifts, indicating that the impact of Bi ions on the states of Co and Mn ions is not obvious.

2.3. Electrochemical Performance

The rate performance of VNMC, 1BiNMC, and 3BiNMC is shown in Figure 4. In Figure 4a, VNMC delivers an initial charge capacity of 230 $mAhg^{-1}$ and discharge capacity of 204 $mAhg^{-1}$, which is comparable to previous works.[35,36] When 0.1 mol% Bi ions are added, the initial charge and discharge specific capacities of 1BiNMC are 246.1 and 222.9 $mAhg^{-1}$, respectively, which are 16.1 and 18.9 $mAhg^{-1}$ higher than that of VNMC. When the concentration of Bi ions increases to 0.3 mol%, the initial charge capacity is 237 $mAhg^{-1}$ and discharge specific capacity is 212.5 $mAhg^{-1}$, which are slightly higher than that of VNMC, but lower than that of 1BiNMC.

The same trend can also be observed at different current density. In Figure 4b, VNMC delivers specific rate capacity of 195.35, 181.35, 165.71, 152.88, 138.93,128.53, and 111.83 $mAhg^{-1}$ with the current density of 0.1, 0.2, 0.5, 1.0, 2.0, 3.0, and 5.0 C, respectively. For 1BiNMC, it exhibits a specific capacity of 211.88, 203.18, 191.93, 182.67, 172.81, 165.71, and 155.23 $mAhg^{-1}$ from 0.1 to 5.0 C, respectively, which are 16.5~43.4 $mAhg^{-1}$ higher than VNMC. When the Bi content increases to 0.3 mol%, the specific capacities of 3BiNMC at each current density (200.28, 189.26, 176.81, 166.69, 155.76, 146.46, 131.49 $mAhg^{-1}$) are also larger than that of VNMC, but not as obvious as 1BiNMC. The difference of capacity retention (Figure S6a) and specific capacity (Figure 4c, 4d and S6b) among Bi modified samples and VNMC gradually become obvious with the increase of current rate. The variations in specific capacity observed among these samples are primarily attributed to differences in the degree of cation mixing and the lattice parameters of each sample. As indicated in the XRD refinement results, 1BiNMC and 3BiNMC exhibit a lower degree of cation mixing than VNMC, enhancing Li^+ transfer and specific capacity. Meanwhile, the lattice parameter of 1BiNMC and 3BiNMC are larger than that of VNMC, enabling fast Li^+ diffusion and high specific capacity at high rates.[31] The fast Li^+ diffusion of 1BiNMC also can be contributed by the radial orientation of primary particles because of the short Li^+ diffusion path. Meanwhile, CVC mode is employed to preserve electrochemical equilibrium in the overvoltage state, which occurs due to polarization of the electrodes in the CC mode.[37] The higher percentage of capacity generation in the CVC mode represents the increasing polarization. The CVC capacity and percentage of CVC capacity in total charge capacity are shown in Figure S6c and Figure 4e. The percentage of CVC capacity in 1BiNMC is much lower than that in VNMC, indicating the lower polarization of 1BiNMC. Thus, due to the low polarization, 1BiNMC delivers better rate performance than VNMC.

To compare the Li^+ diffusion among VNMC and 1BiNMC, the Li^+ diffusion coefficient (D_{Li}) during charge and discharge process is tested by GITT and CV. As shown in Figure 4f and

Research Article
doi.org/10.1002/batt.202400107
Chemistry Europe
European Chemical Societies Publishing

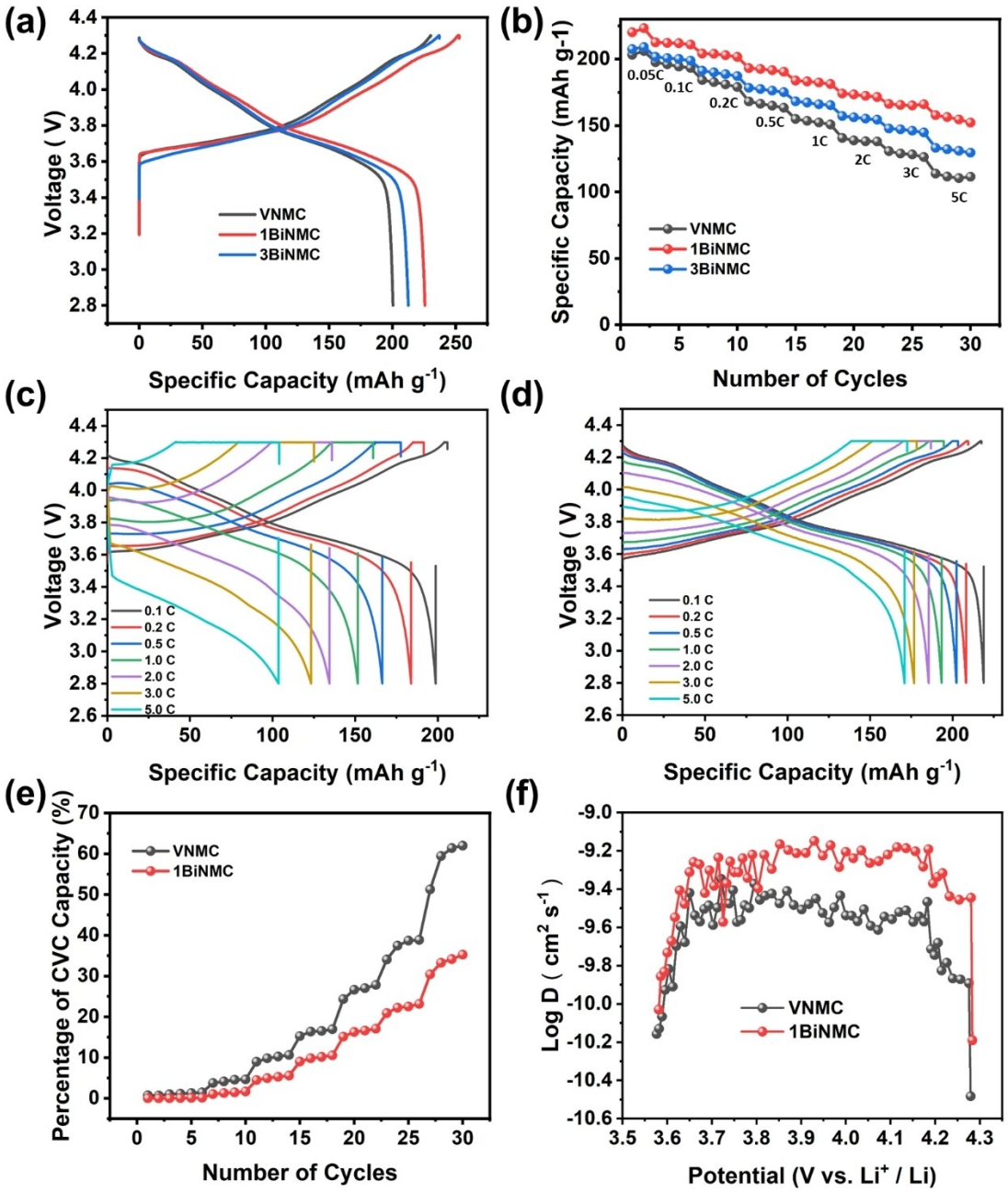

Figure 4. Rate performance of VNMC, 1BiNMC, and 3BiNMC. (a) First charge/discharge profiles; (b) rate performance between 2.8 and 4.3 V; (c) the capacity voltage curves with different current rate of VNMC; (d) the capacity voltage curves with different current rate of 1BiNMC; (e) the percentage of CVC capacity in the total specific charge capacity; (f) Li^+ diffusion coefficients determined through GITT analysis during charge.

Figure S6d, 1BiNMC delivers higher $D_{Li,}$ than VNMC. Meanwhile, in Figure S7a and S7b, through a series of CV tests at various scan rates, D_{Li} also can be determined. In Figure S7c and S7d, the anodic and cathodic slopes corroborate a strong correlation between anodic and cathodic diffusivity, representing the Li^+ diffusion during delithiation and lithiation, respectively.[38] The D_{Li} values of VNMC are calculated to be 2.35×10^{-10} cm^2/s (anodic) and 9.40×10^{-11} cm^2/s (cathodic), which is comparable to previous works.[6] The D_{Li} of 1BiNMC are 6.50×10^{-10} cm^2/s (anodic) and 2.29×10^{-10} cm^2/s (cathodic), which are about 2.8 and 2.4 times higher than the D_{Li} of VNMC, respectively, suggesting that 1BiNMC is able to demonstrate superior electrochemical performance compared to VNMC.

The cycling performance of cathode materials is measured with full cells at 0.33 C from 2.5 to 4.2 V (vs. graphite), as shown in Figure 5a and b. At the 1st cycle with 0.33 C, VNMC delivers a specific discharge capacity of 183.3 $mAhg^{-1}$, and after 100 cycles, the specific capacity drops to 143.9 $mAhg^{-1}$, with a capacity retention of 78.51 %. After Bi ions are added, 1BiNMC and 3BiNMC deliver the specific capacity of 196.30 and 184.80 $mAhg^{-1}$ at 1st cycle and a reserved capacity of 171.65 and 154.7 $mAhg^{-1}$ at 100th cycle, respectively. The capacity

Research Article
doi.org/10.1002/batt.202400107
Chemistry Europe
European Chemical Societies Publishing

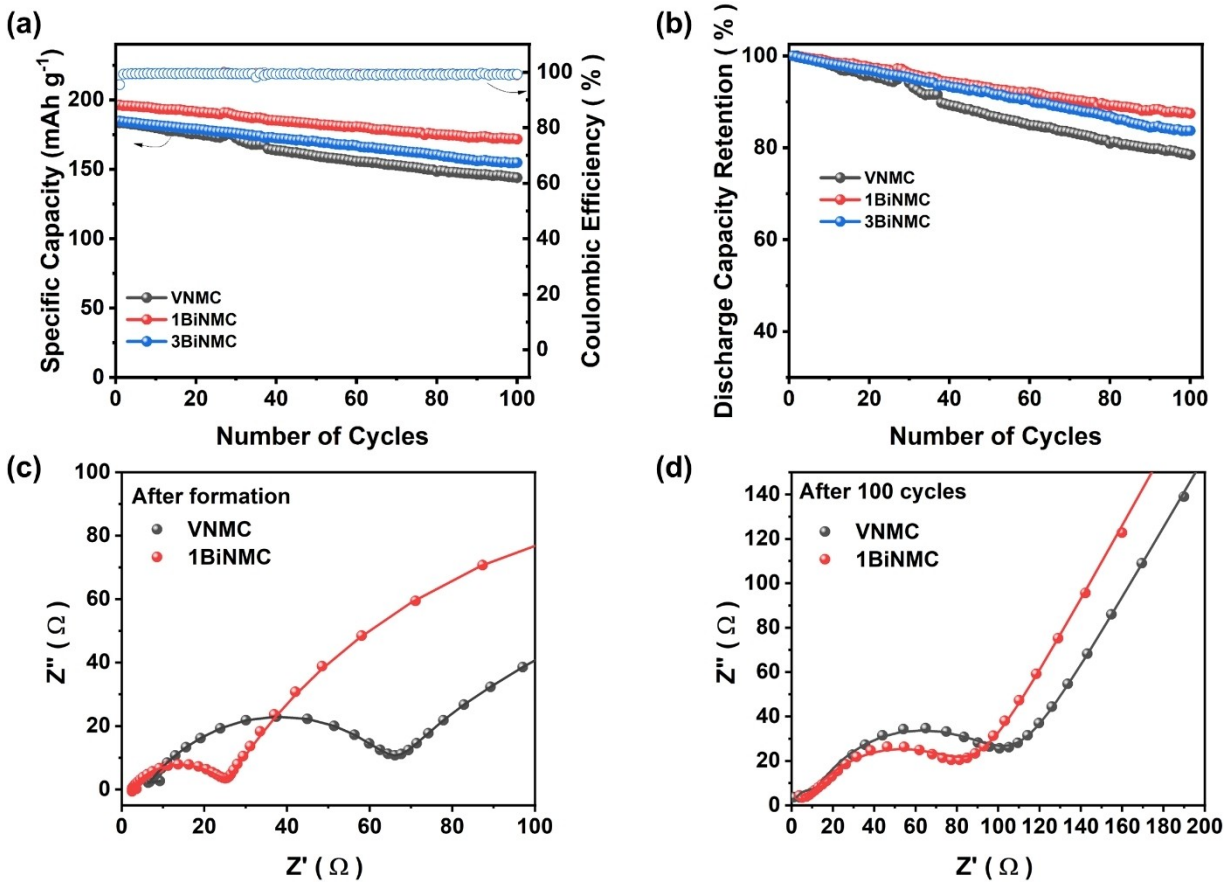

Figure 5. Cycle performance of VNMC, 1BiNMC, and 3BiNMC. (a) Cycling performances; (b) capacity retention; (c) EIS plots of VNMC and 1BiNMC after formation; (d) EIS plots of VNMC and 1BiNMC after 100 cycles.

retention of 1BiNMC and 3BiNMC are 87.44% and 83.71%, respectively. Specifically, 1BiNMC delivers the highest retention capacity after 100 cycles, 27.75 $mAhg^{-1}$higher than VNMC, representing the optimized cycling stability. The enhanced cycle stability of 1BiNMC can be attributed to its improved structural stability due to its low degree of cation mixing, resulting in the optimized capacity retention during cycling. Meanwhile, the increasing rate of capacity fading is also relevant to the growing cell polarization, which is corresponding to the rise or fall in the median charge or discharge voltage during cycling.[6] The capacity voltage curves of VNMC and 1BiNMC with different cycles are shown in Figure S8a and b. VNMC exhibits significant voltage attenuation and capacity degradation during cycling, while the voltage attenuation and capacity degradation of 1BiNMC are not such obvious.

To investigate the impact of Bi ions on ionic conduction during cycling, VNMC and 1BiNMC are tested by EIS after formation and cycling (100 cycles). According to the fitted data in Table S4, the Rs values for all the cells remain relatively stable throughout the test duration, demonstrating that the conductivity of electrolyte are not influenced by the Bi ions.[39] However, the difference in the R_{ct} between VNMC and 1BiNMC is obvious. For VNMC, the R_{ct} after formation and after 100 cycles are 7.61 Ω and 61.71 Ω while the R_{ct} of 1BiNMC after formation and after 100 cycles are 3.36 Ω and 47.58, respectively. 1BiNMC exhibits a smaller semicircle (Figure 5c and 5d) and R_{ct} than VNMC, representing the effects of Bi on limiting the charge transfer resistance.

2.4. Degradation Analysis

To probe possible degradation mechanisms, the dQ/dV profiles of VNMC and 1BiNMC are presented in Figure S8c and d, which represent the phase transitions during cycling. At around 4.2 V, The phase transition occurring (from H2 to H3 phase) is widely recognized as causing significant lattice shrinkage/expansion along the c-axis, leading to mechanical strain and capacity degradation.[40] The voltage difference of this peak between 1st cycle to 100th cycle for 1BiNMC is 0.21 V, which is half of that for VNMC (0.43 V), indicating that the characteristic peak indicative the H2 to H3 phase transition of in 1BiNMC exhibits greater reversibility during cycling. Thus, the mechanical integrity of the particles is preserved, enabling the material to maintain its specific discharge capacity. Meanwhile, this trend also can be found in the results of CV test results. The CV curves of the first 5 cycles are shown in Figure S9a and b, where the peak-to-peak width of H2 to H3 redox pair increases more rapidly than VNMC, indicating that the irreversibility of the transition in VNMC is faster than that in 1BiNMC.

Research Article
doi.org/10.1002/batt.202400107
Chemistry Europe
European Chemical Societies Publishing

To further probe the structural change during lithiation/delithiation process, ex situ XRD at 4.3 V was performed for both VNMC and 1BiNMC. Typically, the shift in the (003) peak is associated with the intercalation and deintercalation of Li^+ during the lithiation/delithiation process. During charging, Li^+ ions migrate out of the cathode structures towards the anode side, causing the (003) peak shift towards a lower angle. As shown in Figure 6a and b, for 1BiNMC, the (003) peak shift is much smaller than that for VNMC. Since this peak shift is indicative of changes in the c-direction, the smaller shift observed in the 1BiNMC electrode suggests that its crystal structure experiences less contraction in the c-direction.[41,42] Meanwhile, based on Figure 6c, 6d, S10a, and S10b, even in the first charge process, cracks can be observed in VNMC, while there is no crack in 1BiNMC. Therefore, 1BiNMC possesses a more stable structure than VNMC during lithiation/delithiation process.

The changes in crystal structures of VNMC and 1BiNMC after 100 cycles are also measured by Ex-situ XRD. As displayed in Figure 6e and f, the clearly splitting of (108)/(110) and (006)/(102) peaks of 1BiNMC indicates the well crystalline layered structure after 100 cycles, while due to the unclear splitting of (108)/(110) and unsplit (006)/(102) peaks, VNMC cannot maintain the well crystalline layered structure after 100 cycles. The seriously destroyed layer structure is due to the phase transition from H2 to H3, and the well-maintained layer structure in

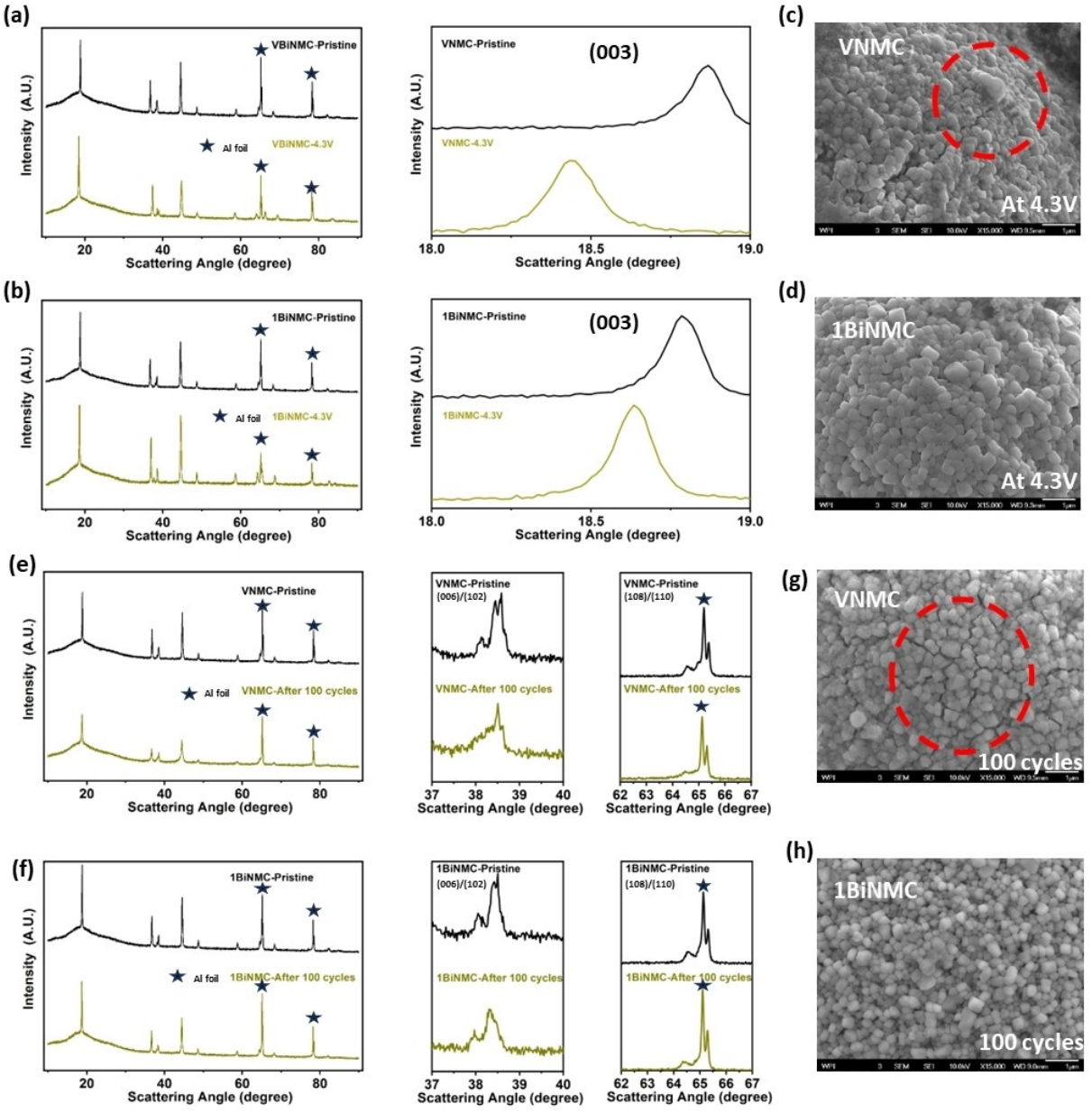

Figure 6. Ex-situ structural characterizations of VNMC, 1BiNMC, and 3BiNMC. Ex Situ XRD pattern with enlarged (006)/(102) and (108)/(110) peak position of electrodes before and after charging to 4.3 V of (a) VNMC and (b) 1BiNMC. SEM images of electrodes charging to 4.3 V of (c) VNMC and (d) 1BiNMC. Ex Situ XRD pattern with enlarged (006)/(102) and (108)/(110) peak position of electrodes before and after 100 cycles of (e) VNMC and (f) 1BiNMC. SEM images of electrodes 100 cycles of (g) VNMC and (h) 1BiNMC.

1BiNMC is primarily attributed to the stronger TM–O bonds resulting from the substitution of Bi ions into Ni sites, which stabilizes the structure and inhibits the phase transition from H2 to H3 in a highly delithiated state.[15,17, 43] Moreover, large number of cracks can be found on VNMC after 100 cycles while cracks are hardly observed on 1BiNMC, as shown in Figure 6g, 6h, S10c, and S10d. The obvious difference also can be attributed to the Bi_2O_3 coating which can effectively prevent limit the corrosion and damage from electrolyte.[18] According to the ex-situ XRD and SEM results, 1BiNMC retains much greater structural crystallinity and morphology after the long cycling than VNMC. According to the results mentioned above, the incorporation of Bi ions can enhance the electrochemical performance of NMC cathode via stabilizing the structure and limiting the contraction in c-direction during lithiation/delithiation process.

3. Conclusions

Bi modified NMC cathodes were successfully synthesized through a facile solid-state reaction from metal oxide, lithium hydroxide and hydroxide precursors. The effects of Bi substitution on the morphology, crystal structure, and electrochemical performance of the NMC cathodes were discovered. It was found that 0.1 mol% Bi substitution(1BiNMC) can significantly improve the rate and cycling performance of unmodified NMC(VNMC). 1BiNMC delivers striking rate capacities, even 43.4 $mAhg^{-1}$ higher than VNMC at 5 C. Meanwhile, 1BiNMC provides capacity retention of 87.44% after 100 cycles, ~10% higher than VNMC. The impressive electrochemical performance of the Bi modified NMC cathodes benefits from the role of Bi in improving Li^+ diffusion, structural stability, and cracking resistance during lithiation/delithiation process. Therefore, the effective Bi modification provides a possible solution to optimizing the electrochemical performance of Ni-rich cathodes.

Supporting Information

Supporting Information is available from the Wiley Online Library or from the author.

Acknowledgements

Z. Meng and J. Hou contributed to this work equally. Argonne National Laboratory's work, XPS testing, was supported by the U.S. Department of Energy, Vehicle Technologies Office, under contract DE-AC02-06CH11357.

Conflict of Interests

The authors declare no conflict of interest.

Data Availability Statement

The data that support the findings of this study are available from the corresponding author upon reasonable request.

Keywords: Lithium-ion battery · Ni-rich cathode materials · Bi modification · structural stability

[1] W. Li, E. M. Erickson, A. Manthiram, *Nat. Energy* **2020**, *5*(1), 26–34. DOI: 10.1038/s41560-019-0513-0.
[2] Q. Liu, X. Su, D. Lei, Y. Qin, J. Wen, F. Guo, Y. A. Wu, Y. Rong, R. Kou, X. Xiao, et al., *Nat. Energy* **2018**, *3*(11), 936–943. DOI: 10.1038/s41560-018-0180-6.
[3] P. Vanaphuti, Y. Liu, X. Ma, J. Fu, Y. Lin, J. Wen, Z. Yang, Y. Wang, *ACS Appl. Mater. Interfaces* **2021**, *13*(19), 22597–22607. DOI: 10.1021/acsami.1c04718.
[4] P. Vanaphuti, J. Bai, L. Ma, S. Ehrlich, K. Kisslinger, F. Wang, Y. Wang, *Energy Storage Mater.* **2020**, *31*, 459–469. DOI: 10.1016/j.ensm.2020.08.003.
[5] A. Manthiram, J. B. Goodenough, *Nat. Energy* **2021**, *6*(3), 323–323. DOI: 10.1038/s41560-020-00764-8.
[6] L. Azhari, Z. Meng, Z. Yang, G. Gao, Y. Han, Y. Wang, *J. Power Sources* **2022**, *545*. DOI: 10.1016/j.jpowsour.2022.231963.
[7] P. Vanaphuti, Z. Cui, A. Manthiram, *Adv. Funct. Mater.* 2308619. DOI: 10.1002/adfm.202308619.
[8] Z. Meng, X. Ma, L. Azhari, J. Hou, Y. Wang, *Communications Materials* **2023**, *4*(1), 90. DOI: 10.1038/s43246-023-00418-8.
[9] M. Jiang, D. L. Danilov, R. A. Eichel, P. H. Notten, *Adv. Energy Mater.* **2021**, *11*(48), 2103005.
[10] L. Ni, S. Zhang, A. Di, W. Deng, G. Zou, H. Hou, X. Ji, *Adv. Energy Mater.* **2022**, *n/a*, 2201510, https://doi.org/10.1002/aenm.202201510. DOI: https://doi.org/10.1002/aenm.202201510 (acccessed 2022/07/09).
[11] H.-H. Ryu, K.-J. Park, C. S. Yoon, Y.-K. Sun, *Chem. Mater.* **2018**, *30*(3), 1155–1163. DOI: 10.1021/acs.chemmater.7b05269.
[12] T. R. Tanim, P. J. Weddle, Z. Yang, A. M. Colclasure, H. Charalambous, D. P. Finegan, Y. Lu, M. Preefer, S. Kim, J. M. Allen, et al., *Adv. Energy Mater.* **2022**, *12*(46), 2202795. DOI: 10.1002/aenm.202202795.
[13] Y. Lu, T. Zhu, E. McShane, B. D. McCloskey, G. Chen, *Small* **2022**, *18*(12), 2105833. DOI: 10.1002/smll.202105833.
[14] B. P. Thapaliya, S. Misra, S.-z. Yang, C. J. Jafta, H. M. Meyer III, P. Bagri, R. R. Unocic, C. A. Bridges, S. Dai, *Adv. Mater. Interfaces* **2022**, *9*(18), 2200035. DOI: 10.1002/admi.202200035.
[15] H. Lv, C. Li, Z. Zhao, B. Wu, D. Mu, *J. Energy Chem.* **2021**, *60*, 435–450. DOI: 10.1016/j.jechem.2021.01.044.
[16] L. Qiu, M. Zhang, Y. Song, Z. Wu, Y.-F. Zhu, J. Zhang, D. Wang, H.-Y. Hu, H.-W. Li, H.-R. Liu, et al., *Carbon Energy* **2023**, *5*(7), 298. DOI: 10.1002/cey2.298.
[17] Y. Jiang, F. Guo, L. Qiu, T. Liu, Y. Hu, W. Yang, Y. Liu, Y. Sun, Z. Wu, Y. Song, et al., *ACS Appl. Mater. Interfaces* **2023**, *15*(29), 35072–35081. DOI: 10.1021/acsami.3c07022.
[18] Y. Liu, T. Zeng, G. Li, T. Wan, M. Li, X. Zhang, M. Li, M. Su, A. Dou, W. Zeng, et al., *Energy Storage Mater.* **2022**, *52*, 534–546. DOI: 10.1016/j.ensm.2022.08.026.
[19] X. Qu, H. Huang, T. Wan, L. Hu, Z. Yu, Y. Liu, A. Dou, Y. Zhou, M. Su, X. Peng, et al., *Nano Energy* **2022**, *91*, 106665. DOI: 10.1016/j.nanoen.2021.106665.
[20] W. Yan, S. Yang, Y. Huang, Y. Yang, Y. Guohui, *J. Alloys Compd.* **2020**, *819*. DOI: 10.1016/j.jallcom.2019.153048.
[21] Z. Ahaliabadeh, X. Kong, E. Fedorovskaya, T. Kallio, *J. Power Sources* **2022**, *540*, 231633. DOI: 10.1016/j.jpowsour.2022.231633.
[22] L. Zhou, H. Wu, M. Tian, Q. Zheng, C. Xu, D. Lin, *RSC Adv.* **2016**, *6*(74), 6979–69797. DOI: 10.1039/c6ra14087d.
[23] Y. Hao, W. Liu, Q. Zhang, X. Wang, H. Yang, L. Kou, Z. Tian, L. Shao, H. Maleki Kheimeh Sari, J. Wang, et al., *Nano Energy* **2021**, *88*, 106240. DOI: 10.1016/j.nanoen.2021.106240.
[24] S. Zhang, G. Hu, K. Du, Z. Peng, L. Li, Y. Zhang, Y. Cao, *Electrochim. Acta* **2023**, *470*, 143280. DOI: 10.1016/j.electacta.2023.143280.
[25] Y. Zhou, H. Zhang, Y. Wang, T. Wan, P. Guan, X. Zhou, X. Wang, Y. Chen, H. Shi, A. Dou, et al., *ACS Nano* **2023**, *17*(20), 20621–20633. DOI: 10.1021/acsnano.3c07655.
[26] J. Liang, Y. Lu, J. Wang, X. Liu, K. Chen, W. Ji, Y. Zhu, D. Wang, *J. Energy Chem.* **2020**, *47*, 188–195. DOI: 10.1016/j.jechem.2019.12.009.

[27] R. Zhang, Z. Meng, X. Ma, M. Chen, B. Chen, Y. Zheng, Z. Yao, P. Vanaphuti, S. Bong, Z. Yang, et al., *Nano Energy* **2020**, *78*, 105214. DOI: 10.1016/j.nanoen.2020.105214.
[28] C. Wan, L. Zhao, C. Wu, L. Lin, X. Liu, *J. Cleaner Prod.* **2022**, *380*, 135005. DOI: 10.1016/j.jclepro.2022.135005.
[29] X. Ma, P. Vanaphuti, J. Fu, J. Hou, Y. Liu, R. Zhang, S. Bong, Z. Yao, Z. Yang, Y. Wang, *Nano Energy* **2021**, *87*. DOI: 10.1016/j.nanoen.2021.106194.
[30] J. Wang, C. Liu, G. Xu, C. Miao, M. Wen, M. Xu, C. Wang, W. Xiao, *Chemical Engineering Journa* **2022**, *438*, 135537. DOI: 10.1016/j.cej.2022.135537.
[31] F. Li, Z. Liu, J. Shen, X. Xu, L. Zeng, B. Zhang, H. Zhu, Q. Liu, J. Liu, M. Zhu, *J. Mater. Chem. A* **2021**, *9*(5), 2830–2839. DOI: 10.1039/d0ta10608a.
[32] G. Mao, J. Luo, Q. Zhou, F. Xiao, R. Tang, J. Li, L. Zeng, Y. Wang, *Nanoscale* **2021**, *13*(44), 18741–18753, 10.1039/D1NR06005H. DOI: 10.1039/D1NR06005H.
[33] G. Sathishkumar, C. Venkataraju, R. Murugaraj, K. Sivakumar, *J. Mater. Sci. Mater. Electron.* **2012**, *23*(1), 243–250. DOI: 10.1007/s10854-011-0395-9.
[34] Y. Liu, L.-b. Tang, H.-x. Wei, X.-h. Zhang, Z.-j. He, Y.-j. Li, J.-c. Zheng, *Nano Energy* **2019**, *65*. DOI: 10.1016/j.nanoen.2019.104043.
[35] H. Wu, X. Pang, J. Bi, L. Wang, Z. Li, L. Guo, H. Liu, Q. Meng, H. Jiang, C. Liu, et al., *J. Alloys Compd.* **2020**, *829*, 154571. DOI: 10.1016/j.jallcom.2020.154571.
[36] M. Zhang, C. Wang, J. Zhang, G. Li, L. Gu, *ACS Omega* **2021**, *6*(25), 16465–16471. DOI: 10.1021/acsomega.1c01552.
[37] Y. Lee, C. Park, K. Park, *Chem. Mater.* **2024**, *36*(1), 232–246. DOI: 10.1021/acs.chemmater.3c01998.
[38] Y. Zheng, R. Zhang, P. Vanaphuti, Y. Liu, Z. Yang, Y. Wang, *ACS Appl. Mater. Interfaces* **2021**, *13*(48), 57171–57181. DOI: 10.1021/acsami.1c17341.
[39] P. Thanwisai, P. Vanaphuti, Z. Yao, J. Hou, Z. Meng, X. Ma, H. Guo, G. Gao, Z. Yang, Y. Wang, *Small* **2024**,*20(9),* 2306465. DOI: 10.1002/smll.202306465.
[40] Q. Li, R. Dang, M. Chen, Y. Lee, Z. Hu, X. Xiao, *ACS Appl. Mater. Interfaces* **2018**, *10*(21), 17850–17860. DOI: 10.1021/acsami.8b02000.
[41] J. Li, R. Shunmugasundaram, R. Doig, J. R. Dahn, *Chem. Mater.* **2016**, *28*(1), 162–171. DOI: 10.1021/acs.chemmater.5b03500.
[42] L. Qiu, W. Xiang, W. Tian, C.-L. Xu, Y.-C. Li, Z.-G. Wu, T.-R. Chen, K. Jia, D. Wang, F.-R. He, et al., *Nano Energy* **2019**, *63*, 103818. DOI: 10.1016/j.nanoen.2019.06.014.
[43] L. Qiu, Y. Song, M. Zhang, Y. Liu, Z. Yang, Z. Wu, H. Zhang, W. Xiang, Y. Liu, G. Wang, et al., *Adv. Energy Mater.* **2022**, *12*(19), 2200022. DOI: 10.1002/aenm.202200022.

Manuscript received: February 17, 2024
Revised manuscript received: March 31, 2024
Accepted manuscript online: April 10, 2024
Version of record online: May 7, 2024